Detrended fluctuation analysis of the magnetic and electric field variations that precede rupture

P. A. Varotsos, N. V. Sarlis, and E. S. Skordas
Solid State Section and Solid Earth Physics Institute, Physics Department, University of Athens, Panepistimiopolis, Zografos 157 84, Athens, Greece

(Received 2 January 2009; accepted 17 April 2009; published online 18 May 2009)

Magnetic field variations are detected before rupture in the form of "spikes" of alternating sign. The distinction of these spikes from random noise is of major practical importance since it is easier to conduct magnetic field measurements than electric field ones. Applying detrended fluctuation analysis (DFA), these spikes look to be random at short time lags. On the other hand, long-range correlations prevail at time lags larger than the average time interval between consecutive spikes with a scaling exponent α around 0.9. In addition, DFA is applied to recent preseismic electric field variations in long duration (several hours to a couple of days) and reveals a scale invariant feature with an exponent $\alpha \approx 1$ over all scales available (around five orders of magnitude).
 [DOI: 10.1063/1.3130931]

Many physical and biological complex systems exhibit scale-invariant features characterized by long-range power-law correlations, which are often difficult to quantify due to the presence of erratic fluctuations, heterogeneity, and nonstationarity embedded in the emitted signals. Here, we focus on different types of nonstationarities such as random spikes and pseudosinusoidal trends that may affect the long-range correlation properties of signals that precede rupture. Since these nonstationarities may either be epiphenomena of external conditions or may arise from the intrinsic dynamics of the system, it is crucial to distinguish their origin. This is attempted in the present paper for both the magnetic and the electric field variations that appear before rupture by employing the detrended fluctuation analysis (DFA) as a scaling method to quantify long-range temporal correlations. In particular, for the magnetic field variations which have usually the form of "spikes" of alternating sign, we find that at short time scales they look to be random (thus may then be confused with random noise), but at larger scales long-range correlations prevail. As for the electric field variations with long duration (up to a couple of days), which are usually superimposed on a pseudosinusoidal background, a scale-invariant feature over five orders of magnitude with an exponent close to unity has been found.

I. INTRODUCTION

The DFA[1–9] is a novel method that has been developed to address the problem of accurately quantifying long-range correlations in nonstationary fluctuating signals. It has been already applied to a multitude of cases including DNA,[10–13] human motor activity[14] and gait,[15,16] cardiac dynamics,[17–20] meteorology,[21,22] and climate temperature fluctuations.[23] Traditional methods such as power spectrum and autocorrelation analysis[24] are not suitable for nonstationary signals.[5,9]

DFA is, in short, a modified root-mean-square (rms) analysis of a random walk and consists of the following steps. Starting with a signal $u(i)$, where $i=1,2,\ldots,N$, and N is the length of the signal, the first step is to integrate $u(i)$ and obtain

$$y(i) = \sum_{j=1}^{i} [u(j) - \bar{u}], \tag{1}$$

where $\bar{u}$ stands for the mean

$$\bar{u} = \frac{1}{N}\sum_{j=1}^{N} u(j). \tag{2}$$

We then divide the profile $y(i)$ into boxes of equal length n. In each box, we fit $y(i)$ using a polynomial function $y_n(i)$, which represents the local trend in that box. (If a different order l of polynomial fit is used, we have a different order DFA-l, for example, DFA-1 if $l=1$, DFA-2 if $l=2$, etc.) Next, the profile $y(i)$ is detrended by subtracting the local trend $y_n(i)$ in each box of length n,

$$Y_n(i) = y(i) - y_n(i). \tag{3}$$

Finally, the rms fluctuation for the integrated and detrended signal is calculated,

$$F(n) \equiv \sqrt{\frac{1}{N}\sum_{i-1}^{N} [Y_n(i)]^2}. \tag{4}$$

The behavior of $F(n)$ over a broad number of scales is obtained by repeating the aforementioned calculation of $F(n)$ for varied box length n. For scale invariant signals, we find

$$F(n) \propto n^{\alpha}, \tag{5}$$

where α is the scaling exponent. If $\alpha=0.5$, the signal is uncorrelated (white noise), while if $\alpha>0.5$ the signal is correlated.[5–9]

By employing the DFA method it was found[25,26] that long-range correlations exist in the original time series of the so-called seismic electric signal (SES) activities, which are low frequency (≤ 1 Hz) electric signals preceding earthquakes.[27–32] The generation of SES is suggested as follows.[39] A change in pressure affects the thermodynamic parameters for the formation, migration, or activation, in general, of defects in solids.[33] In an ionic solid doped with aliovalent impurities a number of extrinsic defects are produced[34,35] for charge compensation, a portion of which is attracted by nearby aliovalent impurities, thus forming electric dipoles that can change their orientation in space through a defect motion.[36,37] Hence, pressure variations may affect the thermodynamic parameters of this motion, resulting in a decrease or increase[38] in the relaxation time of these dipoles, i.e., their (re)orientation takes place faster or slower when an external electric field is applied. When the pressure or the stress, in general, reaches a *critical* value[39] a *cooperative* orientation of these electric dipoles occurs, which results in the emission of a transient electric signal. This may happen in the focal region of a (future) earthquake since the stress gradually should change there *before* rupture.

It has been shown[40,41] that SES activities are better distinguished from electric signals emitted from man-made sources if DFA is applied to a signal after it has been analyzed in a newly introduced time domain, termed natural time χ. In a time series comprising N events, the natural time $\chi_k = k/N$ serves as an index[25] for the occurrence of the kth event. The evolution of the pair (χ_k, Q_k) is studied,[25,31,40–44] where Q_k denotes a quantity proportional to the *energy* released in the kth event. For dichotomous signals, which are frequently the case of SES activities, the quantity Q_k can be represented by the duration of the kth pulse. The normalized power spectrum $\Pi(\omega) \equiv |\Phi(\omega)|^2$ was introduced, where

$$\Phi(\omega) = \sum_{k=1}^{N} p_k \exp\left(i\omega\frac{k}{N}\right) \tag{6}$$

and $p_k = Q_k / \sum_{n=1}^{N} Q_n$, $\omega = 2\pi\phi$; ϕ stands for the *natural frequency*. In natural time analysis, the properties of $\Pi(\omega)$ or $\Pi(\phi)$ are studied for natural frequencies ϕ less than 0.5, since, in this range of ϕ, $\Pi(\omega)$ or $\Pi(\phi)$ reduces to a *characteristic function* for the probability distribution p_k in the context of probability theory. When the system enters the critical stage, the following relation holds:[25,31]

$$\Pi(\omega) = \frac{18}{5\omega^2} - \frac{6\cos\omega}{5\omega^2} - \frac{12\sin\omega}{5\omega^3}. \tag{7}$$

For $\omega \to 0$, Eq. (7) leads to[25]

$$\Pi(\omega) \approx 1 - 0.07\omega^2,$$

which reflects[31] that the variance of χ is given by

$$\kappa_1 \equiv \langle \chi^2 \rangle - \langle \chi \rangle^2 = 0.07,$$

where $\langle f(\chi) \rangle = \sum_{k=1}^{N} p_k f(\chi_k)$. The entropy S in the natural time domain is defined as[41]

$$S \equiv \langle \chi \ln \chi \rangle - \langle \chi \rangle \ln \langle \chi \rangle,$$

which depends on the sequential order of events.[42] It exhibits[43] concavity, positivity, Lesche[45,46] stability, and for SES activities (critical dynamics) its value is smaller[41] than the value $S_u (= \ln 2/2 - 1/4 \approx 0.0966)$ of a "uniform" (u) distribution, as defined in Refs. 40–42, e.g., when all p_k are equal or Q_k are positive independent and identically distributed random variables of finite variance (i.e., coming from the same probability density function of finite variance). In this case, κ_1 and S are designated κ_u ($=1/12$) and S_u, respectively. Thus, $S < S_u$. The same holds for the value of the entropy obtained[43,44] upon considering the time reversal $\hat{T}$ (the operator $\hat{T}$ is defined by $\hat{T} p_\kappa = p_{N-k+1}$), which is labeled by S_-. In summary, the SES activities, in contrast to the signals produced by man-made electrical sources when analyzed in natural time, exhibit *infinitely* ranged temporal correlations[40,41] and obey the conditions[44]

$$\kappa_1 = 0.07 \tag{8}$$

and

$$S, S_- < S_u. \tag{9}$$

For major earthquakes, i.e., with magnitude Mw6.5 or larger, SES activities are accompanied[47] by detectable variations in the magnetic field B.[48] These variations, when measured by coil magnetometers, have the form of spikes of alternating sign. It is therefore of interest to investigate whether these spikes exhibit long-range temporal correlations. This investigation, which is of major importance since only magnetic field data are usually available in most countries[28,49,50] (since it is easier to conduct magnetic field measurements than electric field ones), is made here in Sec. II.

In the up to date applications of DFA, long-range correlations have been revealed in SES activities of duration up to a few hours.[25,26,40,41] During the last few years, however, SES activities of appreciably longer duration, i.e., from several hours to a couple of days, have been collected. These data now enable the investigation of scaling in a wider range of scales than hitherto known. This provides an additional scope of the present paper and is carried out in Sec. III. A discussion of the results concerning the magnetic and electric data follows in Sec. IV. Finally, our conclusions are presented in Sec. V.

II. MAGNETIC FIELD VARIATIONS PRECEDING RUPTURE

The measurements have been carried out by three DANSK coil magnetometers oriented in East-West (EW), North-South (NS), and vertical directions. The calibration of these magnetometers[47,51] showed that for periods larger than around half a second, the magnetometers measure the time derivative dB/dt of the magnetic field and their output is "neutralized" at $\sim$200 ms after the "arrival" of a Heaviside unit step magnetic variation. It means that a signal recorded by these magnetometers should correspond to a magnetic variation that has "arrived" at the sensor less than 200 ms before the recording. The data were collected by a Campbell 21X datalogger with sampling frequency $f_{\exp} = 1$ sample/s.

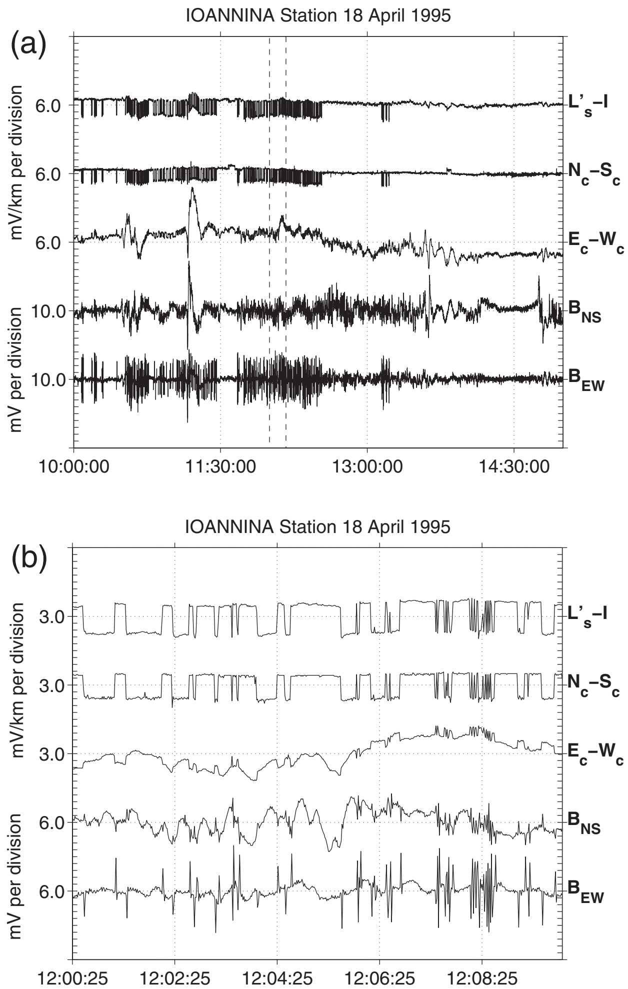

FIG. 1. (a) Variations in the electric (upper three channels) and magnetic (lower two channels) fields recorded on April 18, 1995 (see text). (b) A 10 min excerpt of (a). The two dashed lines in (a) show the excerpt depicted in (b).

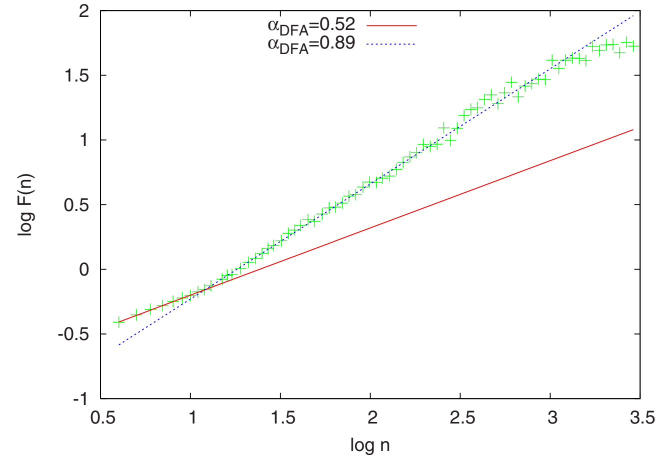

FIG. 2. (Color online) The DFA for the B_{EW} channel of Fig. 1(a). Logarithm base 10 is used.

Figure 1(a) provides an example of simultaneous recordings on April 18, 1995 at a station located close to Ioannina (IOA) city in northwestern Greece. Variations in both the electric (E) and magnetic field (B) are shown. They were followed by a magnitude Mw6.6 earthquake (the Centroid Moment Tensor solutions reported by the United States Geological Survey) with an epicenter at 40.2 °N 21.7 °E, which occurred almost 3 weeks later, i.e., on May 13, 1995. The recordings of the two horizontal magnetometers oriented along the EW and NS directions, labeled B_{EW} and B_{NS}, are shown in the lower two channels. They consist of a series of spikes of alternating sign, as more clearly seen in a 10 min excerpt of these recordings in Fig. 1(b). These spikes are superimposed on a background which exhibits almost pseudosinusoidal magnetotelluric (MT) variations in duration much larger than 1 s which are induced by frequent small variations in the Earth's magnetic field. In addition, the horizontal variations were monitored at the same station by measuring the variation ΔV of the potential difference between (pairs of) electrode-measuring dipoles that are grounded at depths of ~ 2 m. Several such dipoles were deployed along the EW and NS directions with lengths (L) a few to several tens of meters (short dipoles) or a couple of kilometers (long dipoles). The electric field is given by $E = \Delta V / L$ and is usually measured in mV/km. For example, the data from the following measuring dipoles are shown in the upper three channels of Fig. 1(a): two short electric dipoles at site c of IOA station (see the supplementary information of Ref. 47 as well as Ref. 52 where the selection of site c has been discussed) of length 50 m (E_c-W_c and N_c-S_c having different records because they are oriented[52] along and perpendicular to the local current channeling, respectively) and a long dipole (L'_s-I) with length of ~ 5 km at an almost NS direction. As it becomes obvious in Fig. 1(b), the E variations consist of a series of almost rectangular pulses (cf. the initiation and cessation of each rectangular pulse correspond to two spikes with opposite sign in the B recordings).

We now apply DFA to the original time series of the magnetic field variations and focus our attention on the B_{EW} component where the intensity of spikes is higher. Dividing the time series of length N into N/n nonoverlapping fragments, each with n observations, and determining the local trend of the subseries, we find the corresponding log $F(n)$ versus log(n) plot where $n = f_{exp}\ \Delta t$, as shown in Fig. 2. (Recall that the sampling frequency is $f_{exp} = 1$ sample/s.)

If we fit the data with two straight lines (which are also depicted in Fig. 2) the corresponding scaling exponents are $\alpha = 0.52 \pm 0.04$ and $\alpha = 0.89 \pm 0.03$ for the short-time and long-time lags (i.e., smaller than ~ 12 s and larger than ~ 12 s), respectively. The crossover occurs at a value ($\Delta t \sim 12$ s), which is roughly equal to the average duration $\langle T \rangle \approx 11.01 \pm 0.03$ of each electric pulse, corresponding to the interval between two consecutive alternating spikes. Thus, Fig. 2 shows that at time-lags Δt larger than $\langle T \rangle$ long-range power-law correlations prevail (since $\alpha > 0.5$), while at shorter time lags the α value is very close to that ($\alpha = 0.5$) of an uncorrelated signal (white noise).

The above findings are reminiscent of the case of signals with superposed *random* spikes studied by Chen *et al.*[7] They reported that for a correlated signal with spikes, they found a crossover from uncorrelated behavior at small scales to cor-

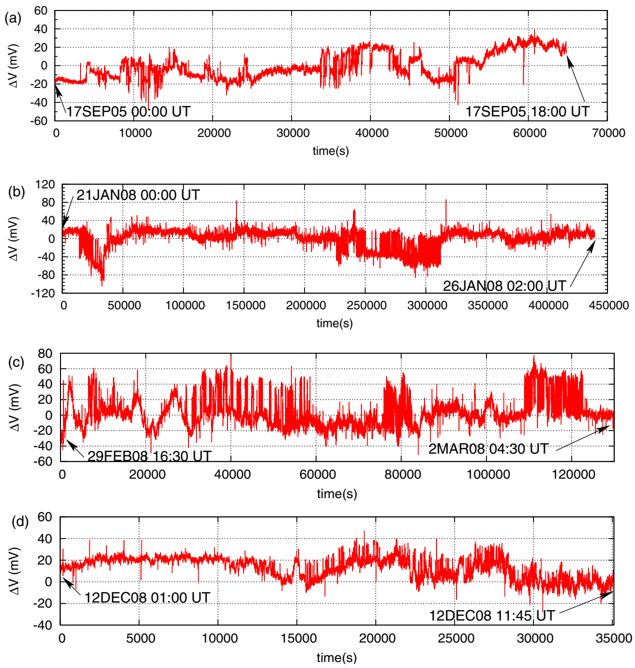

FIG. 3. (Color online) Long duration SES activities during the last few years (see text).

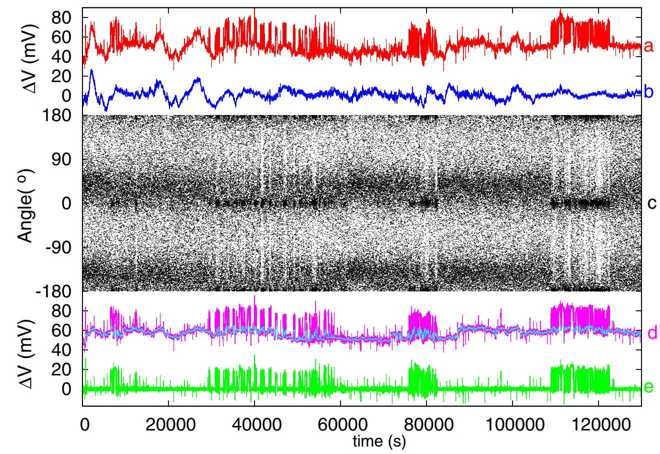

FIG. 4. (Color online) The long duration SES activity from February 29 to March 2, 2008. Channel a: original time series; Channel b: recordings at a measuring dipole which did not record the SES activity but show MT variations; Panel c: the angle of the resulting vector upon assuming that the 1 s increments of channel a lie along the x-axis and those of channel b along the y-axis; Channel d: the residual of a linear least-squares fit of channel a with respect to channel b; Channel e: the same as d but after eliminating the slight variations in the MT background. For the sake of clarity, channels a, b, and d have been shifted vertically.

related behavior at large scales with an exponent close to the exponent of the original stationary signal. They also investigated the characteristics of the scaling of the spikes only and found that the scaling behavior of the signal with random spikes is a superposition of the scaling of the signal and the scaling of the spikes. The case studied by Chen *et al.*,[7] however, is different from the present case, because the spikes studied here correspond to the preseismic magnetic field variations and hence are *not* random [cf. recall that when applying DFA to the "durations" of the electric field rectangular pulses shown in Fig. 1(b), we found[40] an exponent around 1].

III. DFA OF SES ACTIVITIES OF LONG DURATION

In Fig. 3, the following four long duration SES activities are depicted *all* of which have been recorded with sampling frequency $f_{\exp}=1$ sample/s at a station close to Pirgos city located in western Greece. At this station only electric field variations are continuously monitored with a multitude of measuring dipoles.[53] First, the SES activity on September 17, 2005 with duration of several hours that preceded the Mw6.7 earthquake with an epicenter at 36.3 °N 23.3 °E on January 8, 2006. Second, the SES activity that lasted from January 21 until January 26, 2008 and preceded the Mw6.9 at 36.5 °N 21.8 °E on February 14, 2008. Third, the SES activity during the period from February 29 to March 2, 2008 that was followed[32] by a Mw6.4 earthquake at 38.0 °N 21.5 °E on June 8, 2008. Finally, Fig. 3(d) depicts the most recent SES activity of duration of several hours which was recorded on December 12, 2008. This last SES activity was followed by a Mw5.4 earthquake at 37.1 °N 20.8 °E on February 16, 2009. Note that this earthquake occurred after the initial submission of the present paper, while its time of occurrence was predicted[54] on February 5, 2009 by means of the procedure developed in Ref. 32.

Here, we analyze as an example the long duration SES activity that lasted from February 29 until March 2, 2008 [Fig. 3(c)]. The time series of this electrical disturbance, which is not of obvious dichotomous nature, is reproduced in channel "a" of Fig. 4. The signal, comprising a number of pulses, is superimposed on a background which exhibits frequent small MT variations. The latter are simultaneously recorded at all measuring sites, in contrast to the SES activities that solely appear at a restricted number of sites depending on the epicentral region of the future earthquake.[39] This difference provides a key for their distinction. In order to separate the MT background, we proceed in the following steps. First, we look into the simultaneous data of another measuring dipole of the same station, i.e., the data shown in channel "b" in Fig. 4, which has not recorded the signal but does show the MT pseudosinusoidal variations. Second, since the sampling rate of the measurements $f_{\exp}$ is one sample/s, we now read the increments every 1 s of the two time series of channels a and b. Placing the "1 s increments" of channel a along the x-axis and those of b along the y-axis, we obtain increment vectors and plot in the middle panel "c" of Fig. 4 their angles with dots. When a non-MT variation (e.g., a dichotomous pulse) appears (disappears) in channel a, the angle in c abruptly changes to 0° (±180°). Thus, the dots in panel c mark such changes. In other words, an increased density of dots (dark regions) around 0° or ±180° marks the occurrence of these pulses on which we should focus. To this end, we plot, in channel "d" of Fig. 4 the residual of a linear least-squares fit of channel a with respect to channel b. Comparing channel d with channel a, we notice a significant reduction in the MT background but not of the signal. The small variations in the MT background which still remain in d are now marked by the light blue line. When this is re-

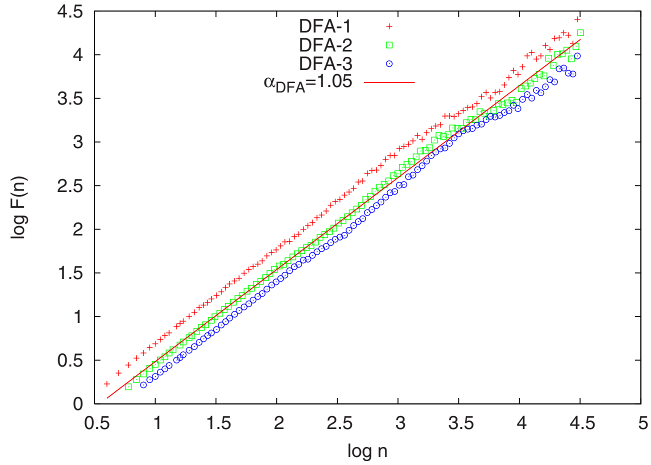

FIG. 5. (Color online) The DFA-l (l=1, 2, and 3) for the lower channel (i.e., the one labeled e) of Fig. 4. Logarithm base 10 is used.

moved, channel d results in channel e. Hence, channel e solely contains the electric field variations that precede rupture. This channel provides the time series which should now be analyzed.

The DFA analysis (in conventional time) of the time series of channel "e" of Fig. 4 is shown in Fig. 5. It reveals an almost linear $\log F(n)$ versus $\log n$ plot (where $n = f_{\exp}\Delta t$) with an exponent $\alpha \approx 1$ practically over all scales available (approximately five orders of magnitude). Note that this value of the exponent remains the same irrespective if we apply DFA-1, DFA-2, or DFA-3. This result is in agreement with the results obtained[25,26,40,41] for SES activities of *shorter* duration.

In order to distinguish whether the signal in Fig. 4 is a true SES activity or a man-made electric signal, we now proceed to its analysis in natural time. To obtain the time series (χ_k, Q_k), the individual pulses of the signal depicted in channel e of Fig. 4 have to be identified. A pulse starts, of course, when the amplitude exceeds a given threshold and ends when the amplitude falls below it. Moreover, since the signal is not obviously dichotomous, instead of finding the duration of each pulse, one should sum the "instantaneous

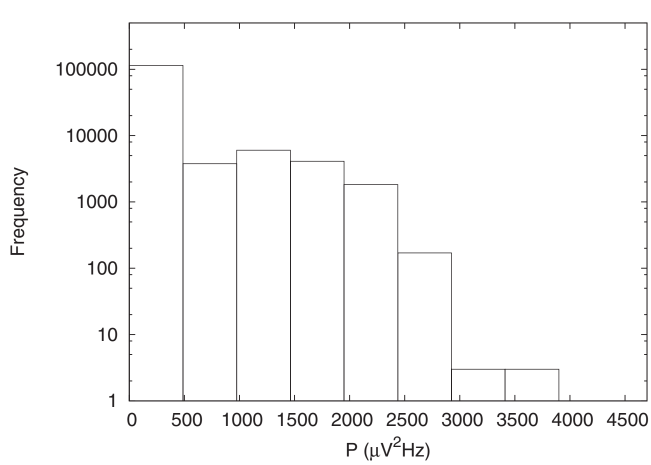

FIG. 6. Histogram of the instantaneous power P, i.e., the squared amplitude of the signal depicted in channel e of Fig. 4.

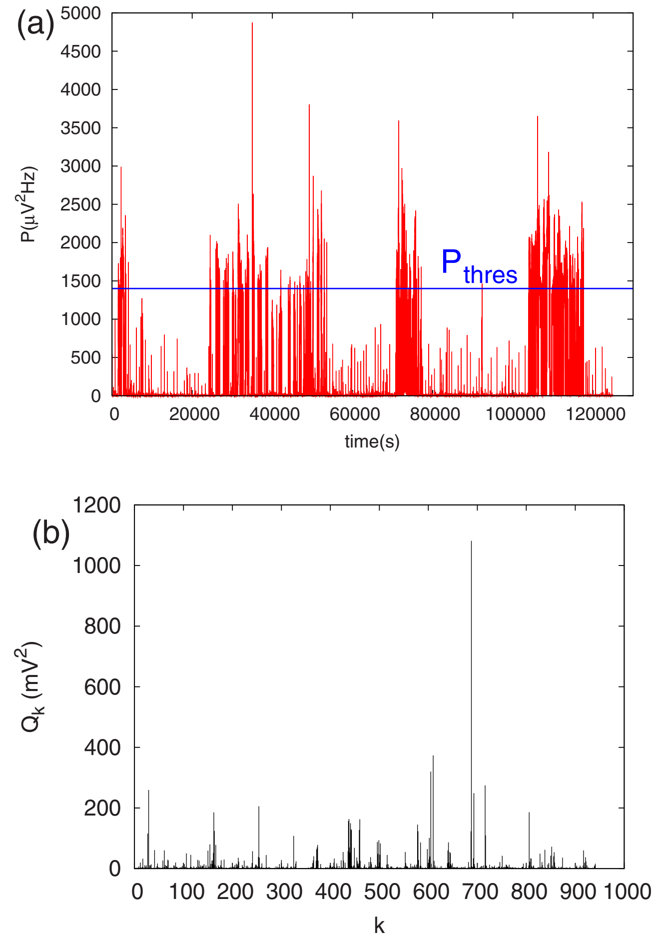

FIG. 7. (Color online) (a) The instantaneous power P of the signal depicted in channel e of Fig. 4 (computed by squaring its amplitude). The solid line parallel to the x-axis marks an example of a threshold P_{thres}(=1400 μV^2 Hz) chosen. (b) The resulting representation of the signal depicted in channel e of Fig. 4 in natural time when considering P_{thres}=1400 μV^2 Hz.

power" during the pulse duration in order to find Q_k. To this end, we plot in Fig. 6 the histogram of the instantaneous power P of channel e of Fig. 4, computed by squaring its amplitude. An inspection of this figure reveals a bimodal feature which signifies the periods of inactivity ($P < 500$ μV^2 Hz) and activity ($P > 500$ μV^2 Hz) in channel e of Fig. 4. In order to find Q_k, we focus on the periods of activity and select the power threshold P_{thres} around the second peak of the histogram in Fig. 6. Let us consider, for example, the case of P_{thres}=1400 μV^2 Hz. In Fig. 7(a), we depict the instantaneous power P of the signal in channel e of Fig. 4. Starting from the beginning of the signal, we compare P with P_{thres} and when P exceeds P_{thres} we start summing up the P values until P falls below P_{thres} for the first time, k=1. The resulting sum corresponds to Q_1. This procedure is repeated until P falls below P_{thres} for the second time, k=2, and the new sum represents Q_2, etc. This leads to the natural time representation depicted in Fig. 7(b). The result depends, of course, on the selection of P_{thres}. The proper selection can be verified by checking whether a small change in P_{thres} around the second peak of the histogram in Fig. 6 leads to a natural time representation resulting in approximately the same values of the parameters κ_1, S, and S_-. By randomly selecting P_{thres} in the range of 500–2000 μV^2 Hz, we obtain that the number of pulses in channel e of Fig. 4 is $N=1100\pm500$ with $\kappa_1=0.070\pm0.007$, $S=0.082\pm0.012$, and $S_-=0.078\pm0.006$. When P_{thres} ranges between 1000 and 1500 μV^2 Hz, the corresponding values are $N=1200\pm200$ with $\kappa_1=0.068\pm0.003$, $S=0.080\pm0.005$, and $S_-=0.074\pm0.003$. Thus, we observe that irrespective of the P_{thres} value chosen, the parameters κ_1, S, and S_- obey conditions (8) and (9) which the signal of SES activity must satisfy.

IV. DISCUSSION

In general, electric field variations are interconnected with the magnetic field ones through Maxwell equations. Thus, it is expected that when the former exhibit long-range correlations the same should hold for the latter. This expectation is consistent with the present findings which show that at long time lags, the original time series of both electric and magnetic field variations preceding rupture exhibit DFA exponents close to unity.

This can be verified when data of both electric and magnetic field variations are simultaneously available. This was the case of the data presented in Fig. 1. In many occasions, however, as mentioned in Sec. I, only magnetic field data exist because it is easier to conduct magnetic field measurements than electric field ones. When using coil magnetometers, the magnetic field variations have the form of series of spikes. Whenever the amplitude of these spikes significantly exceeds the pseudosinusoidal variations in the MT background, as in the case of B_{EW} in Fig. 1, a direct application of DFA (see Fig. 2) elucidates the long-range correlations in the magnetic field variations preceding rupture. On the other hand, when considerable pseudosinusoidal MT variations are superimposed, a direct application of DFA is not advisable. One must first subtract the MT variations (following a procedure similar to that used in the electric field data in Fig. 4) and then apply DFA.

The preceding paragraph refers to the analysis of the signal in conventional time. As already shown in Ref. 41, natural time analysis allows the distinction between true SES activities and manmade signals. This type of analysis, however, demands the knowledge on the energy released during each consecutive event. The determination of this energy is easier to conduct in the case of electric field variations. This is so because coil magnetometers, as mentioned in Sec. II, act as dB/dt detectors. When the electric field variations are of clear dichotomous nature, the energy release is proportional to the duration of each pulse.[40,41] On the other hand, in the absence of obvious dichotomous nature, an analysis of the instantaneous power similar to that presented in the last paragraph of Sec. III should be carried out to determine the parameters κ_1, S, and S_- in natural time.

V. CONCLUSIONS

First, DFA was used as a scaling analysis method to investigate long-range correlations in the original time series of the magnetic field variations that precede rupture and have the form of spikes of alternating sign. We find a scaling exponent α close to 0.9 for time lags larger than the average time interval $\langle T \rangle$ between consecutive spikes, while at shorter time lags the exponent is close to 0.5, thus corresponding to uncorrelated behavior.

Second, using electric field data of long duration SES activities (i.e., from several hours to a couple of days) recorded during the last few years, DFA reveals a scale invariant feature with an exponent $\alpha \approx 1$ over all scales available (approximately five orders of magnitude).

[1] C.-K. Peng, J. Mietus, J. M. Hausdorff, S. Havlin, H. E. Stanley, and A. L. Goldberger, Phys. Rev. Lett. **70**, 1343 (1993).
[2] C.-K. Peng, S. V. Buldyrev, S. Havlin, M. Simons, H. E. Stanley, and A. L. Goldberger, Phys. Rev. E **49**, 1685 (1994).
[3] S. V. Buldyrev, A. L. Goldberger, S. Havlin, R. N. Mantegna, M. E. Matsa, C.-K. Peng, M. Simons, and H. E. Stanley, Phys. Rev. E **51**, 5084 (1995).
[4] M. S. Taqqu, V. Teverovsky, and W. Willinger, Fractals **3**, 785 (1995).
[5] P. Talkner and R. O. Weber, Phys. Rev. E **62**, 150 (2000).
[6] K. Hu, P. C. Ivanov, Z. Chen, P. Carpena, and H. E. Stanley, Phys. Rev. E **64**, 011114 (2001).
[7] Z. Chen, P. C. Ivanov, K. Hu, and H. E. Stanley, Phys. Rev. E **65**, 041107 (2002).
[8] Z. Chen, K. Hu, P. Carpena, P. Bernaola, H. E. Stanley, and P. C. Ivanov, Phys. Rev. E **71**, 011104 (2005).
[9] L. Xu, P. C. Ivanov, K. Hu, Z. Chen, A. Carbone, and H. E. Stanley, Phys. Rev. E **71**, 051101 (2005).
[10] S. M. Ossadnik, S. B. Buldyrev, A. L. Goldberger, S. Havlin, R. N. Mantegna, C. K. Peng, M. Simons, and H. E. Stanley, Biophys. J. **67**, 64 (1994).
[11] R. N. Mantegna, S. V. Buldyrev, A. L. Goldberger, S. Havlin, C. K. Peng, M. Simons, and H. E. Stanley, Phys. Rev. Lett. **73**, 3169 (1994).
[12] R. N. Mantegna, S. V. Buldyrev, A. L. Goldberger, S. Havlin, C. K. Peng, M. Simons, and H. E. Stanley, Phys. Rev. Lett. **76**, 1979 (1996).
[13] P. Carpena, P. Bernaola-Galv'an, P. C. Ivanov, and H. E. Stanley, Nature (London) **418**, 955 (2002).
[14] K. Hu, P. C. Ivanov, Z. Chen, M. F. Hilton, H. E. Stanley, and S. A. Shea, Physica A **337**, 307 (2004).
[15] J. M. Hausdorff, Y. Ashkenazy, C. K. Peng, P. C. Ivanov, H. E. Stanley, and A. L. Goldberger, Physica A **302**, 138 (2001).
[16] Y. Ashkenazy, J. M. Hausdorff, P. C. Ivanov, and H. E. Stanley, Physica A **316**, 662 (2002).
[17] P. C. Ivanov, A. Bunde, L. A. Nunes Amaral, S. Havlin, J. Fritsch-Yelle, R. M. Baevsky, H. E. Stanley, and A. L. Goldberger, Europhys. Lett. **48**, 594 (1999).
[18] S. Havlin, S. V. Buldyrev, A. Bunde, A. L. Goldberger, P. C. Ivanov, C. K. Peng, and H. E. Stanley, Physica A **273**, 46 (1999).
[19] H. E. Stanley, L. A. Nunes Amaral, A. L. Goldberger, S. Havlin, P. C. Ivanov, and C. K. Peng, Physica A **270**, 309 (1999).
[20] L. A. Nunes Amaral, A. L. Goldberger, P. C. Ivanov, and H. E. Stanley, Phys. Rev. Lett. **81**, 2388 (1998).
[21] K. Ivanova and M. Ausloos, Physica A **274**, 349 (1999).
[22] K. Ivanova, T. P. Ackerman, E. E. Clothiaux, P. C. Ivanov, H. E. Stanley, and M. Ausloos, J. Geophys. Res., [Atmos.] **108**, 4268 (2003).
[23] E. Koscielny-Bunde, A. Bunde, S. Havlin, H. E. Roman, Y. Goldreich, and H. J. Schellnhuber, Phys. Rev. Lett. **81**, 729 (1998).
[24] R. L. Stratonovich, *Topics in the Theory of Random Noise* (Gordon and Breach, New York, 1981), Vol. I.
[25] P. A. Varotsos, N. V. Sarlis, and E. S. Skordas, Phys. Rev. E **66**, 011902 (2002).
[26] A. Weron, K. Bunecki, S. Mercik, and K. Weron, Phys. Rev. E **71**, 016113 (2005).
[27] P. Varotsos and K. Alexopoulos, Tectonophysics **110**, 73 (1984); P. Varotsos and K. Alexopoulos, *ibid.* **110**, 99 (1984).
[28] A. C. Fraser-Smith, A. Bernardi, P. R. McGill, M. E. Ladd, R. A. Helliwell, and O. G. Villard, Geophys. Res. Lett. **17**, 1465, DOI: 10.1029/GL017i009p01465 (1990).
[29] S. Uyeda, T. Nagao, Y. Orihara, T. Yamaguchi, and I. Takahashi, Proc. Natl. Acad. Sci. U.S.A. **97**, 4561 (2000).
[30] S. Uyeda, M. Hayakawa, T. Nagao, O. Molchanov, K. Hattori, Y. Orihara,

K. Gotoh, Y. Akinaga, and H. Tanaka, Proc. Natl. Acad. Sci. U.S.A. **99**, 7352 (2002).
[31]P. A. Varotsos, N. V. Sarlis, H. K. Tanaka, and E. S. Skordas, Phys. Rev. E **72**, 041103 (2005).
[32]N. V. Sarlis, E. S. Skordas, M. S. Lazaridou, and P. A. Varotsos, Proc. Jpn. Acad., Ser. B: Phys. Biol. Sci. **84**, 331 (2008).
[33]P. Varotsos, K. Alexopoulos, and K. Nomicos, Phys. Status Solidi B **111**, 581 (1982).
[34]D. Kostopoulos, P. Varotsos, and S. Mourikis, Can. J. Phys. **53**, 1318 (1975).
[35]P. Varotsos, J. Phys. Chem. Solids **42**, 405 (1981).
[36]P. Varotsos and K. Alexopoulos, J. Phys. Chem. Solids **41**, 443 (1980).
[37]P. Varotsos and K. Alexopoulos, J. Phys. Chem. Solids **42**, 409 (1981).
[38]P. Varotsos and K. Alexopoulos, Phys. Rev. B **21**, 4898 (1980).
[39]P. Varotsos and K. Alexopoulos, *Thermodynamics of Point Defects and Their Relation with Bulk Properties* (North-Holland, Amsterdam, 1986).
[40]P. A. Varotsos, N. V. Sarlis, and E. S. Skordas, Phys. Rev. E **67**, 021109 (2003).
[41]P. A. Varotsos, N. V. Sarlis, and E. S. Skordas, Phys. Rev. E **68**, 031106 (2003).
[42]P. A. Varotsos, N. V. Sarlis, E. S. Skordas, and M. S. Lazaridou, Phys. Rev. E **70**, 011106 (2004).
[43]P. A. Varotsos, N. V. Sarlis, H. K. Tanaka, and E. S. Skordas, Phys. Rev. E **71**, 032102 (2005).
[44]P. A. Varotsos, N. V. Sarlis, E. S. Skordas, H. K. Tanaka, and M. S. Lazaridou, Phys. Rev. E **73**, 031114 (2006).
[45]B. Lesche, J. Stat. Phys. **27**, 419 (1982).
[46]B. Lesche, Phys. Rev. E **70**, 017102 (2004).
[47]P. A. Varotsos, N. V. Sarlis, and E. S. Skordas, Phys. Rev. Lett. **91**, 148501 (2003).
[48]N. Sarlis and P. Varotsos, J. Geodyn. **33**, 463 (2002).
[49]D. Karakelian, G. C. Beroza, S. L. Klemperer, and A. C. Fraser-Smith, Bull. Seismol. Soc. Am. **92**, 1513 (2002).
[50]O. A. Molchanov, Y. A. Kopytenko, P. M. Voronov, E. A. Kopytenko, T. G. Matiashvili, A. C. Fraser-Smith, and A. Bernardi, Geophys. Res. Lett. **19**, 1495, DOI: 10.1029/92GL01152 (1992).
[51]P. Varotsos, N. Sarlis, and E. Skordas, Proc. Jpn. Acad., Ser. B: Phys. Biol. Sci. **77**, 87 (2001).
[52]P. A. Varotsos, N. V. Sarlis, and E. S. Skordas, Appl. Phys. Lett. **86**, 194101 (2005).
[53]P. A. Varotsos, N. V. Sarlis, E. S. Skordas, H. K. Tanaka, and M. S. Lazaridou, Phys. Rev. E **74**, 021123 (2006).
[54]P. A. Varotsos, N. V. Sarlis, E. S. Skordas, and M. S. Lazaridou, e-print arXiv:cond-mat/0707.3074v3.